GADOLINIUM AND HAFNIUM ALUMINO-BOROSILICATE GLASSES: Gd AND Hf SOLUBILITIES

Donggao Zhao*, L.L. Davis**, Liyu Li**, C.S. Palenik*, L.M. Wang*, D.M. Strachan**, R.C. Ewing*

*Department of Nuclear Engineering and Radiological Sciences and Department of Geological Sciences, University of Michigan, Ann Arbor, Michigan 48109-2104, dzhao@umich.edu

**Pacific Northwest National Laboratory, P.O. Box 999 (K6-24), Richland, Washington 99352

ABSTRACT

The solubilities of Hf and Gd in sodium alumino-borosilicate glasses based on the target compositions were examined and confirmed by electron microprobe analysis. The measured compositions of essentially crystal-free glasses are generally homogeneous and close to the target compositions. Therefore, the solubilities of Gd and Hf in sodium alumino-borosilicate glasses based on the target glass compositions are valid. However, for glasses containing precipitates (crystals grown from the melt) and undissolved HfO_2 with overgrowths, the chemical compositions are often heterogeneous and may be significantly different from the target compositions. Precipitated crystalline phases include a rare earth silicate with the apatite structure ($NaGd_9(Si_{5.25}B)O_{26}$) in a gadolinium sodium alumino-borosilicate glass and a HfO_2 phase in hafnium sodium alumino-borosilicate glasses.

INTRODUCTION

Alumino-borosilicate glasses are proposed waste forms for the immobilization of plutonium-containing waste (this does not include the excess weapons plutonium that is to be converted to a crystalline ceramic) and miscellaneous spent nuclear fuels [1-4]. In the present solubility study, new glass compositions in the four-component system (Na_2O-B_2O_3-Al_2O_3-SiO_2) with neutron absorbers (Gd and Hf) have been synthesized to study the effect of variation of the bulk composition on the solubility of Gd and Hf [5-7]. Gadolinium and Hf solubilities in glasses are investigated because 1) Gd and Hf have high neutron capture cross-sections and are effective neutron absorbers that can be used to prevent criticality events during the storage; 2) Gd^{3+} is a surrogate element for Pu^{3+} [6]; and 3) Hf^{4+} is a surrogate element for Pu^{4+} [7]. Experiments have been performed to evaluate the effects of elements such as Na, Al and B on the solubility of Gd and Hf in the borosilicate glasses [6, 7].

The solubility limit is defined as the highest concentration of an element (e.g., Gd or Hf) in the glass above which crystallization or phase separation occurs [6]. Chemical heterogeneity and mass losses during glass synthesis may affect solubility determination. Therefore, it is necessary to directly determine distributions and contents of each individual element in the glasses and associated precipitated crystals. Electron microbeam techniques, such as electron microprobe analysis (EMPA), backscattered electron (BSE) imaging, and energy dispersive X-ray spectroscopy (EDS) were used. We present the compositional features of representative glasses and precipitated crystals as determined by EMPA.

ANALYTICAL METHODS

The glass synthesis method is described in [6] and [7]. Care was taken to minimize mass loss due to volatilization. Thirteen Gd- or Hf-bearing glass samples, with or without precipitated phase, were studied (Table I). Precipitated crystals in some samples are not homogeneously distributed. Therefore, although optically and by XRD, crystals are known to be present, the shard of glass prepared for EMPA may be crystal-free. In addition, some samples examined here

Table I. Gd- and Hf-bearing sodium alumino-borosilicate glass samples.

Sample #	Description
Al15Gd18	Clear Gd glass. No observable crystals
B15Gd42	Clear Gd glass. No observable crystals
B15Gd48	Clear Gd glass with crystalline phase. Elements in crystals: Si, Al, Na, O and Gd
Na10Gd20	Clear Gd glass. No observable crystals
B15Hf30	Clear Hf glass. No observable crystals
B15Hf31	Clear Hf glass. No observable crystals
Na30Hf30	Clear Hf glass. No observable crystals
Na30Hf34	Clear Hf glass. No observable crystals
Na30Hf35a	Clear Hf glass with no crystals
Na30Hf35b	Different Hf glass from sample Na30Hf35a. Clear glass with euhedral HfO_2 crystals (up to tens of μm in size). Elements confirmed in crystals: Hf and O
PL0.35Hf8a	Clear Hf glass with bladed crystals radiating outward from undissolved HfO_2 particles. Heat-treated for one hour at 1560°C and one hour at 1450°C. Elements confirmed in crystals: Hf and O
PL0.35Hf8b	Hafnium glass with tiny crystals. Heat treated for 30 minutes at 1400°C after initially melted at 1560°C for one hour and one hour at 1450°C. Elements confirmed in crystals: Hf and O
PL0.85Hf32	Clear Hf glass with well-developed, hexagonal crystals. Heat-treated for one hour at 1560°C and three hours at 1350°C. Elements confirmed in crystals: Hf and O

were not formed under the same conditions as the samples used in the solubility study. For example, the Hf-bearing glasses, in particular, were melted for longer times in order to grow the large HfO_2 crystals. The samples were prepared by mounting the glass grains in epoxy resin discs that were polished for determination of chemical composition and crystal morphology using BSE, EDS and EMPA. The size of the glass grains ranged from a few millimeters to up to one centimeter.

Backscattered electron imaging and EDS spectra were used to examine the homogeneity of the glass matrix and precipitated crystals, and to characterize the morphology of precipitated crystals. A four-spectrometer Cameca CAMEBAX electron microprobe analyzer (wavelength dispersive system) was used to determine chemical compositions on the polished surfaces. The Cameca PAP correction routine was used in data reduction. The directly analyzed elements were Si, Al, Na, and Gd/Hf with O obtained by stoichiometry and B obtained by difference. Other elements were excluded because the glass and crystals were synthesized with known elemental contents. During each analytical session, spectrometers were verified for position, and each standard was recalibrated and analyzed prior to analyzing the glass samples. A focused beam in spot mode was not used because the glass samples may be damaged by the electron beam, due to the presence of the light elements, B and Na. Standards were SiO_2 for Si, andalusite (Al_2SiO_5) for Al, albite ($NaAlSi_3O_8$) or jadeite ($NaAlSi_2O_6$) for Na, Gd phosphate ($GdPO_4$) for Gd, and metallic Hf for Hf. Glass standards were not used due to alkali loss.

Different EMPA procedures were tested to search for a proper protocol for analyzing the glass samples. To evaluate potential loss of Na, time scans (counts vs. time plot) were conducted using a beam size of 6 x 6 μm^2, accelerating voltage of 15 kV, beam current of 6 nA, and peak and background counting times of 10 and 5 seconds, respectively. The counts vs. time plots show that the counts from NaKα decrease with time, whereas, counts of AlKα, SiKα and GdLα peaks do not change with time, suggesting that Na loss is a problem at these operating conditions. This was confirmed by analyzing the same spot three times consecutively at the same

conditions. The Na_2O content decreases 0.5 wt % each time, with the first analysis closest to the target composition. Thus, beam size was increased to 15 x 15 μm^2. To eliminate or reduce the effect of count time on alkali loss at the increased beam size, Na was counted for 5 periods and then extrapolated to zero time. However, the correction is negligible. For example, for Al15Gd18, NaKα count rates were 566.64, 576.16, 546.10, 542.59, and 562.13 counts/second for counting period #1 to # 5, with an extrapolated zero time count of 568.43 counts/second. This confirms that Na concentration changed just slightly or not at all with time at these conditions. In summary, in order to minimize volatilization of sodium in glass, enlarged beam sizes, lower beam current and shorter count times were used. The optimized procedure is beam size 15 x 15 μm^2, beam current 6 nA, accelerating voltage 15 kV, peak and background counting times of 10 and 5 seconds, B by difference, and O by charge balance. All the analyses of glass matrices were obtained using this procedure. Chemical compositions of precipitated crystals were obtained under the similar conditions [8].

RESULTS

Characteristics of samples and morphology of precipitated crystals

Gd-bearing glasses. The BSE images show that Gd-bearing glass samples Al15Gd18, B15Gd42 and Na10Gd20 are homogeneous in composition and that there are no crystalline phases present in these samples. However, one Gd-bearing glass, sample B15Gd48, contained abundant precipitated crystals in the glass matrix [8]. The shape of the precipitated phase in B15Gd48 is elongate, acicular, prismatic or dendritic with hexagonal cross-sections, indicating that the phase is crystalline, not amorphous. The precipitated crystals are up to 200 μm in length [8]. In a BSE image of sample B15Gd48 (Figure 1A), the glass matrix in the upper left area is darker than those in the central and lower right areas, suggesting that the glass matrix is not homogeneous. The darker area of the BSE image is enriched in Si, Al and Na, whereas the brighter area is enriched in Gd.

Hf-bearing glasses. The BSE images show that samples B15Hf30, B15Hf31, Na30Hf30, Na30Hf34 and Na30Hf35a do not contain crystalline phases and that the glass matrices appear to be homogeneous in composition. Although the first piece of sample Na30Hf35 (labeled as Na30Hf35a) does not contain crystals, a second glass chip (Na30Hf35b) does contain crystals, suggesting that the precipitated crystals are not homogeneously distributed. The precipitated crystals are 20 μm (Figure 1B), and they surround a bubble in the glass (Figure 1C). The EDS spectra indicate that the crystalline phase in Na30Hf35b contains only Hf and O. In PL0.35Hf8a, crystals were found, but were not common. Almost all the crystals are elongated or needle-like (Figure 1D), probably representing the end-on sections of the platy squares of HfO_2 identified optically and by XRD. In PL0.35Hf8b, crystals are common. In contrast to the crystals in PL0.35Hf8a, the crystals in this grain have two different shapes: one is elongated or needle-like, the same as those in PL0.35Hf8a (not common); the other is micron-sized, undissolved HfO_2 with overgrowths (common) (Figure 1E). Sample PL0.35Hf8b was heated for additional 30 minutes at 1400°C after initially melted at 1560°C for one hour and at 1450°C for one hour for PL0.35Hf8a. The differences in size and crystal morphology are consistent with the different melting times (Table I). From EDS spectra, the precipitated crystals in PL0.35Hf8a and PL0.35Hf8b are composed of Hf and O. Precipitated crystals are also common in PL0.85Hf32, but they are bladed and relatively large as compared with the crystals in PL0.35Hf8a and PL0.35Hf8b (Figure 1F). The precipitated crystals in PL0.85Hf32 also consist of Hf and O.

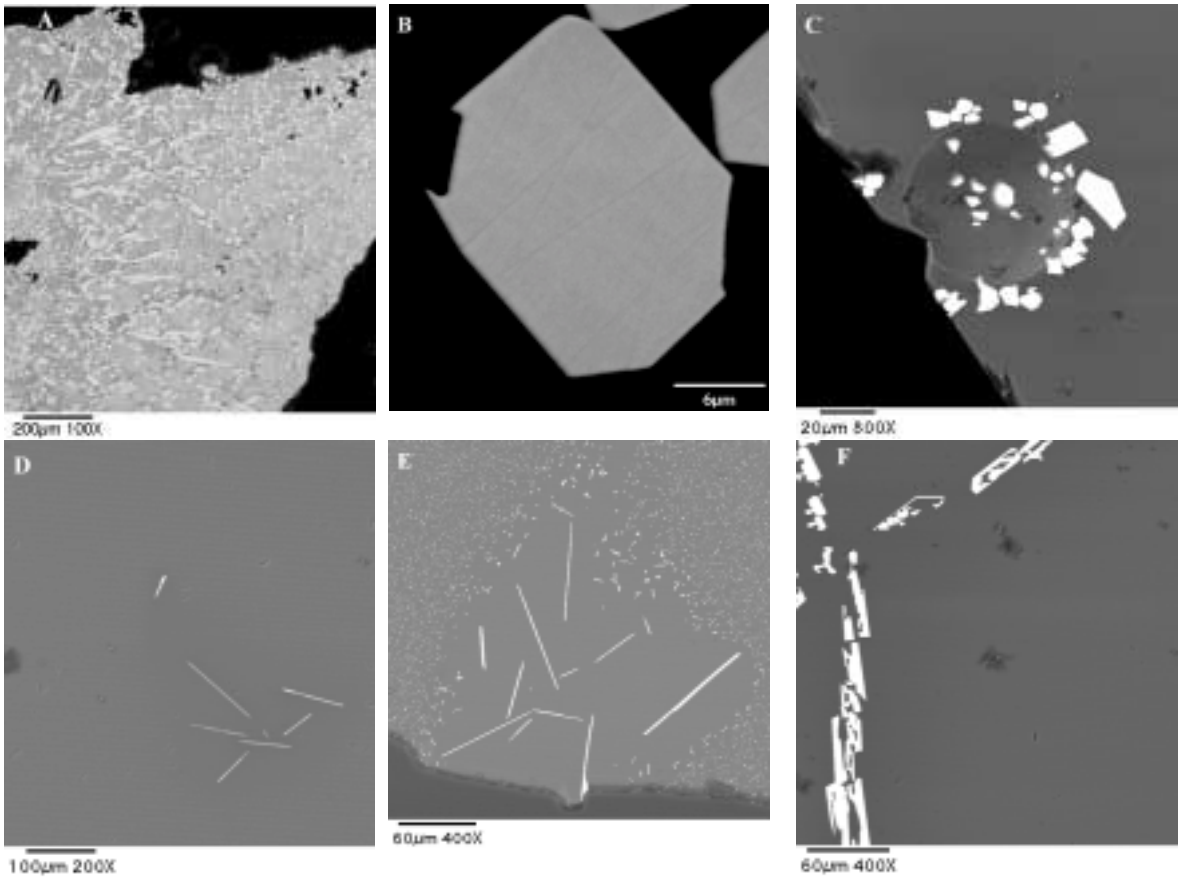

Figure 1. Backscattered electron images of the glass samples containing the precipitated crystalline phases. A) B15Gd48 with elongated, acicular, prismatic or dendritic Gd silicate apatite crystals; cross sections are often hexagonal; glass matrix in the upper left area slightly darker than those in the central and lower right areas, indicating chemical heterogeneity of the matrix. B) Na30Hf35b with euhedral HfO_2 crystals. C) Na30Hf35b with HfO_2 crystals surrounding a bubble in the glass. D) PL0.35Hf8a showing the edges of platy HfO_2 crystals (not common). E) PL0.35Hf8b showing smaller micron-sized, undissolved HfO_2 with overgrowths and edges of larger platy HfO_2 crystals. F) PL0.85Hf32 with bladed HfO_2 crystals.

Chemical compositions of glass matrix

More than one analysis was obtained for each sample. To examine the chemical homogeneity of samples, a few EMPA profiles were completed. Average compositions of sodium alumino-borosilicate glasses are given in Table II.

Homogeneity of glass matrix. The crystal-free Gd-bearing glasses (Al15Gd18, B15Gd42 and Na10Gd20) are homogeneous in chemical composition. In sample B15Gd48, which contains precipitated Gd-rich silicate crystals, two compositional domains were identified in the glass matrix. The glass matrix from the darker upper left area of the BSE image (Figure 1A) is enriched in Si, Al and Na and depleted in Gd, as compared with the glass matrix from the brighter area (Table II; Figure 2). The heterogeneity of the glass matrix in sample B15Gd48 may be caused by crystallization of Gd crystals that take Gd from the glass matrix. Most Hf-bearing glasses are homogeneous in composition. However, the distributions of Hf across the glass grains showed variations. For example, HfO_2 varies significantly in B15Hf31, while Al_2O_3, Na_2O and SiO_2 remain generally constant across the glass grain (Figure 3). Chemical

Table II. Electron microprobe analyses (wt %) of Gd and Hf alumino-borosilicate glasses.

Sample	*Al15Gd18*		*B15Gd42*		*B15Gd48*			*Na10Gd20*		*B15Hf30*	
Point	Ave (7)	Target	Ave (10)	Target	Ave (5)	Ave (4)	Target	Ave (8)	Target	Ave (33)	Target
SiO_2	38.10	39.84	30.94	32.68	28.80	34.04	29.30	47.72	49.90	37.03	39.44
Al_2O_3	16.31	16.91	4.43	4.62	4.30	5.89	4.14	6.86	7.06	5.54	5.58
Na_2O	12.72	13.70	10.90	11.23	10.75	14.02	10.07	7.49	8.58	12.15	13.56
Gd_2O_3	18.90	18.00	42.57	42.00	45.39	31.13	48.00	20.83	20.00	32.02*	30.00*
B_2O_3	13.97	11.55	11.16	9.47	10.75	14.91	8.49	17.10	14.46	13.26	11.42

* Content of HfO_2.

Sample	*B15Hf31*		*Na30Hf30*		*Na30Hf34*		*Na30Hf35*			*PL0.35Hf8*		*PL0.85Hf32*
Point	Ave (35)	Target	Ave (37)	Target	Ave (78)	Target	a Ave (22)	b Ave (41)	Target	a Ave (24)	b Ave (4)	Ave (11)
SiO_2	37.16	38.88	33.67	35.96	30.12	33.90	31.06	30.93	33.39	44.53	47.38	38.75
Al_2O_3	5.53	5.50	5.10	5.08	4.77	4.79	4.73	4.84	4.72	21.53	22.18	6.38
Na_2O	11.66	13.37	17.16	18.54	16.36	17.48	15.74	15.74	17.22	7.21	7.53	11.93
HfO_2	33.05	31.00	32.58	30.00	36.33	34.00	37.79	36.92	35.00	8.40	4.98	29.44
B_2O_3	12.61	11.25	11.49	10.42	12.42	9.83	10.67	11.57	9.67	18.33	17.93	13.50

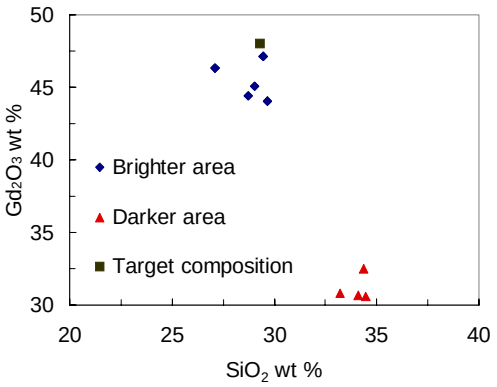

Figure 2. Distributions of SiO_2 and Gd_2O_3 in the glass matrix for B15Gd48 that contains precipitated crystals. Low Gd_2O_3 (31.13 wt %) and high SiO_2 (34.04 wt %) spots are in the darker area of the BSE image (the upper left corner of Figure 1A). High Gd_2O_3 (45.39 wt %) and low SiO_2 (28.80 wt %) spots are in the brighter area (the lower right area of Figure 1A)

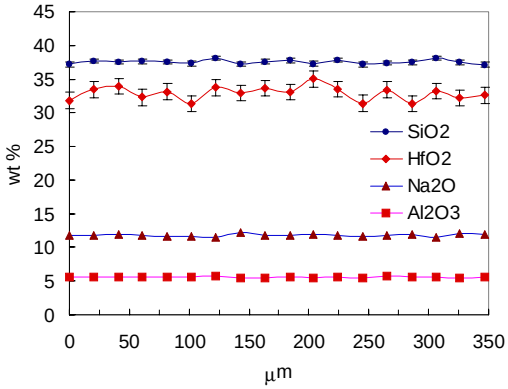

Figure 3. Oxide variations in Hf glass B15Hf31. HfO_2 varies significantly while other oxides remain constant. The profile steps are 20 μm.

compositions of two grains of Na30Hf35 (above the solubility limit) are the same and are close to the target compositions, although one grain contains the crystalline phase HfO_2 (Table II). This suggests that crystallization of small amount of crystals in glass matrix does not change the composition of glass matrix significantly.

Differences between target and measured compositions. For the crystal-free Gd-bearing glasses, such as Al15Gd18, B15Gd42 and Na10Gd20, the measured contents of SiO_2 Al_2O_3 and Na_2O are the same as or slightly lower than those for the target composition; whereas, Gd_2O_3 is

slightly higher. The 1σ uncertainties of measurement are from 0.80 to 1.30 wt % for Gd_2O_3, 0.35 wt % for SiO_2, from 0.10 to 0.20 wt % for Al_2O_3, and from 0.20 to 0.45 wt % for Na_2O. Most differences between target and measured compositions are less than 1 wt %, indicating that the measured and the target compositions are essentially the same (Table II). However, for B15Gd48, which contains precipitated Gd silicate crystals, the differences between the target and the measured compositions are significant. The glass matrix has 31.13 wt % Gd_2O_3 in the darker area and 45.39 wt % Gd_2O_3 in the relatively bright areas (Figure 1A), both different from the 48.00 wt % Gd_2O_3 of the target composition. The composition of the brighter areas is closer to the target composition (Table II). For Hf-bearing glasses without or with a small amount of precipitated HfO_2 crystals, the measured Al_2O_3, SiO_2 and Na_2O are the same as, lower, or slightly lower than those for the target composition. The measured HfO_2 is approximately 2 wt % higher than HfO_2 in the target composition. In general, the measured compositions of Hf-bearing glasses are close to the target compositions, if the glass matrix contains no or only a small amount of precipitated HfO_2 crystals. However, if there are abundant precipitated crystals, the compositions of the glass matrix may vary significantly. For example, in two grains of PL0.35Hf8, the glass matrix with fewer HfO_2 crystals (PL0.35Hf8a) contains 8.40 wt % HfO_2; whereas, the glass matrix with more HfO_2 crystals (PL0.35Hf8b) contains 4.98 wt % HfO_2 (Table II). Measured compositions demonstrate that composition of the glass matrix is the same as or close to the target composition if there are no precipitated crystals or only a small amount of precipitated crystals.

Chemical compositions of precipitated crystals

Precipitated crystals identified in gadolinium alumino-borosilicate glasses (B15Gd48) were described in [8]. The phase is hexagonal, probably a rare earth silicate with the apatite structure $A_{4-x}REE_{6+x}(SiO_4)_{6-y}(PO_4)_y(F,OH,O)_2$ (where A = Li, Na, Mg, Ca, Sr, Ba, Pb and Cd, and REE = La, Ce, Pr, Nd, Pm, Sm, Eu and Gd). The empirical formula is $NaGd_9(Si_{5.25}B)O_{26}$. The presence of B in the precipitated crystals was detected from wavelength dispersive spectrum (WDS) and its contents were obtained by the differences between 100 and the measured totals [8]. For Hf-bearing glasses, the precipitated crystals are HfO_2, as identified by EDS spectra, XRD, and electron microprobe analysis. Due to the small size of the precipitated crystals, detected Si, Al and Na are most likely from the glass matrix. However, the possible existence of these elements and compositional zonings in the HfO_2 crystals are being examined.

CONCLUSIONS

1. Direct measurements of the glass compositions by EMPA demonstrate that glass matrices are homogeneous in chemical composition if there are no or few precipitated crystals. Our EMPA data also show that the measured glass compositions are in general the same as, or close to, the target compositions if there are no or few precipitated crystals.
2. Glass samples with crystals that grew from the melt or abundant undissolved HfO_2 powder are often heterogeneous in chemical composition; and their actual chemical compositions may be significantly different from the target compositions.
3. The precipitated crystalline phase identified in a gadolinium alumino-borosilicate glass is a rare earth silicate apatite; and the precipitated crystals identified in hafnium alumino-borosilicate glasses are HfO_2.
4. Therefore, electron microprobe data confirm that the solubilities of Gd and Hf in sodium alumino-borosilicate glasses based on the target glass compositions are valid if there are no or few precipitated crystals in glass matrices.

ACKNOWLEDGMENT

This study is supported by the Environmental Management Science Program, US Department of Energy through grant # DE-FG07-97-ER45672. The electron microprobe was acquired under Grant # EAR-82-12764 from the National Science Foundation. Liyu Li and Linda L. Davis are grateful to Associated Western Universities for facilitating their postdoctoral appointments at Pacific Northwest National Laboratory.

REFERENCES

1. H. Matzke, J. van Geel, In Disposal of Weapons Plutonium (eds. E.R. Merz and C.E. Walter), Kluwer Academic Publishers, 1996, 93-105.
2. R.C. Ewing, W.J. Weber, W. Lutze, In Disposal of Weapons Plutonium (eds. E.R. Merz and C.E. Walter), Kluwer Academic Publishers, 1996, 65-83.
3. Technical Summary Report for Surplus Weapons-Usable Plutonium Disposition, Report DOE/MD-0003, Office of Fissile Materials Disposition, U.S. Department of Energy, July 17, 1996.
4. L.W. Gray and T.H. Gould, Immobilization Technology Down-Selection Radiation Barrier Approach, Report UCRL-ID-127320, Lawrence Livermore National Laboratory, Livermore, CA, 1997.
5. X. Feng, H. Li, L.L. Davis, L. Li, J.G. Darab, M.J. Schweiger, J.D. Viena, and B.C. Bunker, Distribution and Solubility of Radionuclides in Waste Forms for Distribution of Pu and Spent Nuclear Fuels, Ceramic Transactions, 93, 409-419 (1999).
6. L. Li, D.M. Strachan, H. Li, L.L. Davis, M. Qian, Peraluminous and peralkaline effects on Gd_2O_3 and La_2O_3 solubilities in sodium-alumino-borosilicate glasses, Ceramic Transaction (in press).
7. L. Davis, L. Li, J.G. Darab, H. Li, D. Strachan, P.G. Allen, J.J. Bucher, I.M. Craig, N.M. Edelstein, D.K. Shuh, Scientific Basis for Nuclear Waste Management, XXII, Materials Research Society, Pittsburgh (in press).
8. Donggao Zhao, L.M. Wang, R.C. Ewing, Liyu Li, L.L. Davis, D.M. Strachan, Gd-Apatite Precipitates in a Sodium Gadolinium Alumino-Borosilicate Glass, Journal of Crystal Growth (submitted).